

# $K\bar{K}$ molecules with momentum-dependent interactions

R. H. Lemmer

*School of Physics, University of the Witwatersrand,  
Johannesburg, Private Bag 3, WITS 2050, South Africa*

(Dated: October 26, 2018)

It is shown that the momentum-dependent kaon-antikaon interactions generated via vector meson exchange from the standard  $SU_V(3) \times SU_A(3)$  interaction Lagrangian lead to a non-local potential in coordinate space that can be incorporated without approximation into a non-relativistic version of the Bethe-Salpeter wave equation containing a radial-dependent effective kaon mass appearing in a fully symmetrized kinetic energy operator, in addition to a local potential. Estimates of the mass and decay widths of  $f_0(980)$  and  $a_0(980)$ , considered as  $K\bar{K}$  molecules of isospin 0 and 1, as well as for  $K^+K^-$  atomic bound states (kaonium) are presented, and compared with previous studies of a similar nature. It is argued that without a better knowledge of hadronic form factors it is not possible to distinguish between the molecular versus elementary particle models for the structure of the light scalar mesons.

PACS numbers: 11.10.St, 14.40.Aq, 14.40.Cs, 36.10.-k

arXiv:0902.1739v4 [hep-ph] 24 Oct 2009

Corresponding author: R H Lemmer  
Electronic address: rh\_lemmer@mweb.co.za

## I. INTRODUCTION

The properties of multi quark–antiquark interacting systems as investigated by Weinstein and Isgur [1] pointed to a possible bound kaon–antikaon molecular state structure for the light scalar mesons  $f_0(980)$  and  $a_0(980)$ . Alternative proposals include, in addition to the molecular picture [1, 2, 3, 4, 5, 6], a  $q\bar{q}$  state [7] or a  $q^2\bar{q}^2$  state [8]. However, the large  $2\pi$  annihilation width for  $q\bar{q} \rightarrow \pi\pi \sim 500$  MeV from flux tube–breaking [9] to  $\sim 600$  MeV using current algebra [10], disqualifies a light quark–antiquark configuration when compared with a typical experimental width of  $\sim 50$  MeV for the  $f_0(980) \rightarrow \pi\pi$  decay [11]. The inclusion of strange quarks changes this picture [12, 13]. For example, it is shown in [12] that if the  $f_0(980)$  is identified with the (almost) pure  $s\bar{s}$  member of the nonet within a quark–level linear  $\sigma$  model framework, one can obtain reasonable values for the mass as well as  $\pi\pi$  and  $\gamma\gamma$  decay widths. So the question of a molecular versus a  $q\bar{q}$  elementary particle structure, or perhaps some combination of these, for the light scalars remains an open one [14].

In the following we re–investigate the molecular state option using the non–local extension of the vector meson exchange potentials derived in [5] for kaon–antikaon bound states and their decay modes. It is shown that if one adheres strictly to the approximations required [15, 16] for reducing the instantaneous version of the Bethe–Salpeter equation to a non–relativistic wave equation, especially as regards the off–shell nature of the relative four–momentum of the boson pair undergoing binding, a quantitatively similar picture to that given by a purely local approximation to the potential emerges for kaon–antikaon bound states. In particular, the non–binding states reported in a recent analysis [17] of the same problem now no longer occur.

The paper is arranged as follows: Section II discusses possible kaon–antikaon bound states of the coordinate space version of the non–relativistic Bethe–Salpeter equation for non–local interactions as generated by vector meson exchange from a  $SU_V(3) \times SU_A(3)$  invariant interaction Lagrangian. In Section III we calculate the dominant decay widths of such bound  $K\bar{K}$  pairs of good isospin for annihilation into either  $\pi\pi$  or  $\pi^0\eta$ , while in Section IV the low energy  $K\bar{K}$  scattering parameters in the presence of annihilation are found. Finally, Section V is devoted to a brief discussion of the energy shifts and decay widths to be expected for the associated mesonic atom  $K^+K^-$  (kaonium) in context of the non–local interactions introduced in this paper. A summary and conclusions follow in Section VI.

## II. $K\bar{K}$ BOUND STATES

### A. Non–relativistic Bethe–Salpeter equation

As before [5] we use the non–relativistic version of the Bethe–Salpeter (BS) equation in the instantaneous approximation [15, 16], described further below, to study the mass and decay widths of the  $f_0(980)$  and  $a_0(980)$  scalar mesons, considered as weakly bound kaon–antikaon pairs of isospin zero or one interacting via vector meson exchange. In momentum space this equation reads

$$\left(\frac{\mathbf{p}'^2}{M_K} + 2M_K - P_0\right)\phi(\mathbf{p}') = \frac{1}{4M_K^2} \int \frac{d^3p}{(2\pi)^3} \hat{\Gamma}(\mathbf{p}', \mathbf{p}; P_0)\phi(\mathbf{p}) \quad (1)$$

where  $\phi(\mathbf{p})$  is the wave function of the interacting pair in momentum space;  $M_K \approx 496$  MeV is the average kaon mass. The eigenvalue  $P_0 = 2M_K + E$  is the as yet unknown total mass of the interacting system of binding energy  $E = -\epsilon < 0$ .

Apart from introducing non–relativistic particle propagators, the other essential simplification used in deriving Eq. (1) is the assumption that the interaction is instantaneous. This is implemented by suppressing the time components of the relative four–momenta  $p = (p_1 - p_2)/2 \rightarrow [0, \mathbf{p}]$  and  $p' = (p'_1 - p'_2)/2 \rightarrow [0, \mathbf{p}']$  in the irreducible four–point vertex, or transition amplitude  $(p'_1, p'_2 | \hat{\Gamma} | p_1, p_2)$  of the original BS equation [15]. For a bound state the four–momenta that enter and leave this vertex are all off their mass shell. In the instantaneous approximation in particular this means that  $(p_1, p_2) = [\frac{1}{2}P_0, \pm\mathbf{p}]$  and  $(p'_1, p'_2) = [\frac{1}{2}P_0, \pm\mathbf{p}']$  in the center of mass (c.m.) system, where  $p_1 + p_2 = p'_1 + p'_2 = [P_0, 0]$  still guarantees total energy–momentum conservation for arbitrary values of  $\mathbf{p}$  and  $\mathbf{p}'$ . These approximations result in the transition amplitude

$$(p'_1, p'_2 | \hat{\Gamma} | p_1, p_2) = (p', P_0 | \hat{\Gamma} | p, P_0) \approx \hat{\Gamma}(\mathbf{p}', \mathbf{p}; P_0) \quad (2)$$

which appears in Eq. (1) that only depends on the unconstrained three–momentum of the incoming and outgoing kaons in addition to the total energy, and legitimizes integration over these independent momentum variables.

An expression for  $\hat{\Gamma}(\mathbf{p}', \mathbf{p}; P_0)$  for  $K\bar{K}$  scattering via  $t$ –channel vector meson exchange has been derived in [3, 5] and also [17] from a standard  $SU_V(3) \times SU_A(3)$  invariant interaction Lagrangian [18] to which we refer for further

details. One finds in this case that  $(p'_1, p'_2 | \hat{\Gamma} | p_1, p_2)$  is given to lowest order coupling by

$$(p'_1, p'_2 | \hat{\Gamma} | p_1, p_2) = -g_i^2 C_i n_s \left[ \frac{(p_1 + p'_1) \cdot (p_2 + p'_2) + (p_1^2 - p_1'^2)(p_2^2 - p_2'^2)/M_i^2}{(p_1 - p_1')^2 - M_i^2} \right] \quad (3)$$

that reduces to the approximate transition amplitude introduced in Eq. (2),

$$(p'_1, p'_2 | \hat{\Gamma}_i | p_1, p_2) \approx \hat{\Gamma}_i(\mathbf{p}', \mathbf{p}; P_0) = g_i^2 C_i n_s \left[ \frac{P_0^2 + (\mathbf{p}' + \mathbf{p})^2 + (\mathbf{p}'^2 - \mathbf{p}^2)^2/M_i^2}{(\mathbf{p}' - \mathbf{p})^2 + M_i^2} \right] \quad (4)$$

for the values of the off-shell four-momenta prescribed above. This vertex structure also holds true for  $K\bar{K} \rightarrow \pi\pi$  where  $\mathbf{p}'$  now refers to the outgoing pion momentum, but not for  $K\bar{K} \rightarrow \pi^0\eta$  without modification, see below Eq. (26).

The coupling constants  $g_i^2$  are all related to the the  $\rho\pi\pi$  coupling constant  $g_{\rho\pi\pi}$  by the  $SU(3)$  symmetry [18]:  $g_i^2 = (\frac{1}{4}, \frac{1}{4}, \frac{1}{2})g_{\rho\pi\pi}^2$  for  $i = (\rho, \omega, \phi)$  exchange in  $K\bar{K} \rightarrow K\bar{K}$ , or  $g_i^2 = (g_{\pi KK^*}^2, g_{\pi KK^*}g_{\eta KK^*}) = (\frac{1}{4}, \frac{1}{4}\sqrt{3})g_{\rho\pi\pi}^2$  for  $K^*$  exchange leading to  $K\bar{K} \rightarrow \pi\pi$  or  $\pi^0\eta$  transitions.  $M_i$  is the mass of the exchanged meson in each case, and  $\alpha_s = g_{\rho\pi\pi}^2/4\pi \approx 2.9$  is known from the KSRF relation [19]. The  $C_i = [3, 1, 1]$  or  $[-1, 1, 1]$  are isospin factors [3] for  $(\rho, \omega, \phi)$  exchange between a  $(K\bar{K})_I$  pair coupled to  $I = 0$  or 1, or  $C_i = [-\sqrt{6}, -\sqrt{2}]$  for the  $I = 0$  and 1 transitions  $(K\bar{K})_{0,1} \rightarrow (\pi\pi)_0$  or  $(\pi\eta)_1$  via  $K^*$  exchange;  $(K\bar{K})_1 \rightarrow (\pi\pi)_1$  is forbidden by G parity conservation;  $n_s$  is a symmetry factor  $[\frac{1}{\sqrt{2}}, 1]$  for identical (non-identical) bosons in the final state.

As already remarked in [3], one can check the relations between the various vector-pseudoscalar coupling constants given above empirically by appealing to the experimental decay widths of those vector mesons  $i = (\rho, K^*, \phi)$  that are unstable with respect to decay into  $\pi\pi$ ,  $K\pi$  and  $K\bar{K}$ . An elementary calculation shows that a vector meson of mass  $M_i$  at rest has a decay width of

$$\Gamma_i = n_s^2 f_i \left[ \frac{2}{3} \frac{p_i^3}{M_i^2} \frac{g_i^2}{4\pi} \right] \quad (5)$$

in the scheme of [3] to first order in the relevant coupling constant  $g_i^2$ , where  $p_i$  is the common c.m. momentum magnitude of either decay particle in the final state, and  $f_i = (2, 3, 2)$  an isospin factor for the three channels in question. The symmetry factor  $n_s$  has been defined above. Inserting the known [11] masses and full or partial decay widths of  $(\rho, K^*, \phi)$  as appropriate into Eq. (5), one finds  $(g_{\rho\pi\pi}^2 : g_{\pi KK^*}^2 : g_{\phi K\bar{K}}^2) \sim (1 : (0.54)^2 : (0.77)^2)$  as compared with  $(1 : (1/2)^2 : (1/\sqrt{2})^2)$  given above, where  $g_{\rho\pi\pi}^2/4\pi = 2.92$  that coincides almost exactly with the KSRF value. The remaining empirical ratios hold to within  $\sim 8\%$  of the ‘‘ideal’’ mixing version of the  $SU(3)$  relations between the coupling constants.

The expression for the two-particle vertex given by Eq. (4) regards the basic vertices as point-like. Upon introducing a form-factor depending on the three-momentum transfer  $\mathbf{q} = \mathbf{p}' - \mathbf{p}$  of the form [3]

$$F_i(\mathbf{q}^2) = \left( \frac{2\Lambda^2 - M_i^2}{2\Lambda^2 + \mathbf{q}^2} \right)^2 \quad (6)$$

at each of these vertices with a common high-momentum cutoff  $\sim \sqrt{2}\Lambda$ , the vertex in Eq. (1) is altered to read  $\hat{\Gamma}(\mathbf{p}', \mathbf{p}; P_0) = \sum_i \hat{\Gamma}_i(\mathbf{p}', \mathbf{p}; P_0) F_i^2(\mathbf{q}^2)$ . The use of a common  $\Lambda$  is simply a working assumption; the cutoffs could in principle be different for different vertices [20].

## B. Non-local interaction potential in coordinate space

The vertex in Eq. (4) was approximated further in [5] by neglecting the small binding energy  $\epsilon \sim \frac{1}{50}M_K$  contribution by taking  $P_0 \approx 2M_K$  and ignoring the three-momentum dependence in the numerator entirely. Then the components of the  $K\bar{K}$  potential on the right hand side of Eq. (1) reduce to

$$\frac{1}{4M_K^2} \hat{\Gamma}_i(\mathbf{p}', \mathbf{p}; P_0) F_i^2(\mathbf{q}^2) = g_i^2 C_i U_i(\mathbf{q}), \quad U_i(\mathbf{q}) = \frac{F_i^2(\mathbf{q}^2)}{M_i^2 + \mathbf{q}^2} \quad (7)$$

that is only a function of the momentum transfer  $\mathbf{q}^2$ . This leads to the following set of local potentials in coordinate space for each exchanged meson  $M_i$  that are known in closed form from the fourier transform of  $U_i(\mathbf{q})$ ,

$$V_i(r) = -C_i g_i^2 U_i(r), \quad U_i(r) = \frac{1}{4\pi} \left\{ \frac{e^{-M_i r}}{r} - \frac{e^{-\sqrt{2}\Lambda r}}{r} \sum_{n=0}^3 C_n^{(0)} (\sqrt{2}\Lambda r)^n \right\}. \quad (8)$$

The  $C_n^{(0)}$ 's are polynomials  $C_0^{(0)} = 1$ ,  $C_1^{(0)} = \frac{1}{16}(11 - 4c_i^2 + c_i^4)(1 - c_i^2)$ ,  $C_2^{(0)} = \frac{1}{16}(3 - c_i^2)(1 - c_i^2)^2$  and  $C_3^{(0)} = \frac{1}{48}(1 - c_i^2)^3$  in the variable  $c_i = M_i/\sqrt{2}\Lambda$ . The partial potential  $V_i(r)$  has a simple power series expansion in  $r$  about the origin when the form factor is included,

$$V_i(r) = -\sqrt{2}\Lambda\alpha_i C_i (1 - c_i)^4 \left\{ \frac{1}{16}(5 + 4c_i + c_i^2) - \frac{1}{96}(1 + 4c_i + c_i^2)(\sqrt{2}\Lambda r)^2 + \dots \right\} \quad (9)$$

with  $\alpha_i = g_i^2/4\pi$ , so that the  $V_i(r)$  as well as its space derivatives are all well-behaved at  $r = 0$  for finite  $\Lambda$ .

In general the interaction vertex in Eq. (1) leads to a non-local potential in coordinate space. However, since the numerator in the special case of Eq. (4) is a polynomial in the three-momentum variables, one can incorporate them in coordinate space in a revised potential that also involves space derivatives of  $V_i(r)$  coming from the replacements  $\mathbf{p}$  or  $\mathbf{q} \rightarrow -i\nabla$  in  $\hat{\Gamma}_i(\mathbf{p} + \mathbf{q}, \mathbf{p}; P_0)$ . Again setting  $P_0 \approx 2M_K$ , the  $K\bar{K}$  non-local interaction potential operator  $V_{K\bar{K}}$  becomes

$$V_{K\bar{K}}\psi(r) = V_3(r)\psi(r) - \frac{1}{4M_K^2} \left[ V_2(r)\nabla^2 + 2\nabla \cdot V_2(r)\nabla + \nabla^2 V_2(r) \right] \psi(r) \quad (10)$$

when operating on the  $s$ -state wave function  $\psi(r)$ , the three-dimensional fourier transform of the spherically symmetric momentum space wave function  $\phi(p)$  of Eq. (1).

The potentials  $V_3(r), V_2(r), V_1(r)$  are given by the following combinations (the primes indicate derivatives with respect to  $r$ )

$$\begin{aligned} V_3(r) &= V_1(r) + \frac{1}{2M_K^2} \frac{1}{r} (V_1'(r) - V_2'(r)) \\ V_2(r) &= \sum_i \left( V_i(r) - \frac{V_i''(r)}{M_i^2} \right) \\ V_1(r) &= \sum_i V_i(r). \end{aligned} \quad (11)$$

Then the coordinate space version of Eq. (1) with the full momentum structure of Eq. (4) included can be written as

$$-\frac{1}{4} \left[ \frac{1}{M_K^*(r)} \nabla^2 + 2\nabla \cdot \frac{1}{M_K^*(r)} \nabla + \nabla^2 \frac{1}{M_K^*(r)} \right] \psi(r) + V_3(r)\psi(r) = E\psi(r) \quad (12)$$

containing a spatially-dependent ‘‘effective’’ kaon mass

$$M_K^*(r) = \gamma^{-1}(r)M_K, \quad \gamma(r) = \left( 1 + \frac{V_2(r)}{M_K} \right) \quad (13)$$

that enters into the equation via a fully symmetrized kinetic energy operator.

The quartic terms in the vertex Eq. (4) only contribute to off-shell scattering; they vanish on-shell when  $\mathbf{p}'^2 = \mathbf{p}^2$ . This suggests that their contribution to the interaction potential may be small. If they are omitted entirely, both  $V_3(r)$  and  $V_2(r)$  reduce to  $V_1(r)$  and the structure of Eq. (12) becomes identical in form with that of a wave equation derived in [21] that has been used quite generally for describing non-local effects on particle motion in nuclei [22].

The hermitian structure of the symmetrized kinetic energy operator assures that the eigenstates of Eq. (12) remain orthogonal, and also that the continuity equation for its time-dependent version continues to hold with a revised probability current density  $\mathbf{j}(r, t) = 1/iM_K^*(r)[\psi^* \nabla \psi - \psi \nabla \psi^*]$ . Thus the normalization of  $\psi(r, t)$  also remains independent of time.

### C. Numerical results

We next investigate possible bound  $s$ -state solutions of Eq. (12). It is convenient to set  $\psi(r) = \psi(0)u(r)/r$  with  $u(r)/r \rightarrow 1$  as  $r \rightarrow 0$ . The value of  $\psi(0)$  is fixed by normalization. Then Eq. (12) simplifies to

$$\gamma(r)u'' + \gamma'(r)u' + M_K(E - V_0)u = 0, \quad (14)$$

where

$$V_0(r) = V_1(r) + \frac{1}{2M_K^2} \frac{1}{r} V_1'(r) - \frac{1}{4M_K^2} V_2''(r). \quad (15)$$

We solve this equation numerically after using the partial potentials given by Eq. (8) to construct the required interactions. For  $I = 0$  one has

$$V_1(r) = -g_{\rho\pi\pi}^2 \left( \frac{3}{4}U_\rho(r) + \frac{1}{4}U_\omega(r) + \frac{1}{2}U_\phi(r) \right) \quad (16)$$

and

$$V_2(r) = -g_{\rho\pi\pi}^2 \left[ \frac{3}{4}(U_\rho(r) - \frac{1}{M_\rho^2}U_\rho''(r)) + \frac{1}{4}(U_\omega(r) - \frac{1}{M_\omega^2}U_\omega''(r)) + \frac{1}{2}(U_\phi - \frac{1}{M_\phi^2}U_\phi''(r)) \right] \quad (17)$$

from which  $V_0(r)$  can be obtained. For  $I = 1$  identical expressions hold with the coefficient  $3/4$  of the  $\rho$  meson exchange contribution replaced by  $-1/4$ .

Since known physical masses of exchanged mesons  $(M_\rho, M_\omega, M_\phi) = (768, 783, 1019)$  MeV and their coupling constants given above enter the calculations, the only free parameter is the cutoff  $\Lambda$ . The possible choices of  $\Lambda$  are then restricted further if one in addition requires that  $\gamma(0) > 0$ , in order to ensure that  $M_K^*(r)$  remains positive in the interaction zone [50]. This problem has already been encountered in [17], where it is concluded that for cutoffs that ensure (their equivalent of)  $\gamma(0) > 0$  give non-local potentials that do not bind the  $K\bar{K}$  pair. However these potentials have been based on an approximated vertex that corresponds to  $\hat{\Gamma}_i(\mathbf{p}', \mathbf{p}; P_0)$  of Eq. (4) without the quartic contribution and  $P_0^2$  replaced by the combination  $2(E_{p'}^2 + E_p^2)$  of kaon c.m. energies. The first approximation neglects a small correction term, but the second one excludes off-shell kaons,  $p' \neq p$ , by total energy conservation, contrary to what is expected for bound states. Thus these potentials may not correctly reflect the underlying physics for such systems [15].

This is not the case for the potential operator  $V_{K\bar{K}}$  of Eq. (10). Using Eqs. (9) and (11) one readily finds that

$$\gamma(0) = 1 - \frac{\sqrt{2}\Lambda}{M_K} \sum_i \alpha_i C_i (1 - c_i)^4 \left\{ \frac{1}{16}(5 + 4c_i + c_i^2) + \frac{1}{48}(1 + 4c_i^{-1} + c_i^{-2}) \right\}. \quad (18)$$

For the known interaction strength of  $\alpha_s = g_{\rho\pi\pi}^2/4\pi = 2.9$ , the factor  $\gamma(0)$  stays positive in both isospin channels if  $\Lambda$  lies in the interval  $390 \lesssim \Lambda \lesssim 1280$  MeV, see Fig. 1. However whether or not the resulting non-local potentials bind the  $K\bar{K}$  pair is still sensitive to the actual choice of cutoff. Table I lists calculated values of binding energies, masses and decay half-widths (see next section for the latter) for the subset of cutoff values  $\Lambda = (415, 420, 425)$  MeV confined to a relatively small window within this interval. These cutoffs have been chosen so as to bracket the spread in experimental [11] binding energies  $11.3 \pm 10$  MeV for the  $f_0(980)$  meson considered as an interacting  $K\bar{K}$  pair. As a byproduct the  $a_0(980)$  then also appears as a bound pair state in the isovector channel of these potentials.

A much stronger purely local potential [5] of depth  $\sim 4$  GeV was required to give the same order of binding for  $I = 0$  (and none at all for  $I = 1$ ). The reason for this is clear from Table II which summarizes results for the isoscalar potential. We see that the much shallower non-local potential  $\sim 0.2$  GeV is counter-balanced by a significant suppression of the kinetic energy through an increased effective kaon mass of  $M_K^*(0) \approx 2M_K$  at the origin that favors binding. One notes that cutoff momenta  $q_{max} = \sqrt{2}\Lambda \sim M_\eta$ , of order of the  $\eta$  meson mass, that also sets the mass scale of the pseudo-scalar meson octet, are required to regulate the behavior of the bare vertex in Eq. (4) at large momentum transfer. Otherwise this vertex either tends to a constant or diverges depending on whether the fourth order contribution is dropped or kept. These cutoffs are typically an order of magnitude smaller than those for a local potential like that in Eq. (8) to give the same order of binding. We also comment that the results in Table I remain qualitatively unchanged by dropping the quartic momentum contributions altogether and setting  $V_3(r) = V_2(r) = V_1(r)$  in Eqs. (12) and (13).

### III. DECAY OF $K\bar{K}$ BOUND STATES

The annihilation of bound  $K\bar{K}$  pairs into mesons or photons has been discussed in [5] and [26, 27] in the context of the BS equation. The decay of the bound state is governed by the imaginary part of the additional box diagram  $\hat{\Gamma}_{box}(\mathbf{p}', \mathbf{p}; P_0)$  contribution to the BS equation vertex where a  $K^*$  vector meson is exchanged in the  $t$ -channel, see Fig. 2. Then the eigenvalue  $P_0$  in Eq. (1) acquires an imaginary part,  $P_0 \rightarrow P_0 - i\Gamma/2$ . The imaginary part of the box diagram can be retrieved directly by applying the Cutkosky rules [15] to cut the intermediate meson loops in Fig. 2. The decay widths  $\Gamma$  are then obtained perturbatively by averaging over the bound state solutions of Eq. (1) in the absence of annihilation.

For the  $I = 0$ ,  $K\bar{K} \rightarrow \pi\pi$  decay this width reads

$$\Gamma_{\pi\pi} = \frac{1}{32\pi^2} \frac{p_\pi}{M_K} \frac{1}{4M_K^2} \int d\Omega_\pi |M_B(p_\pi)|^2 \quad (19)$$

where the bound to free transition amplitude  $M_B(p_\pi)$  can be written as either a momentum or a coordinate space integral,

$$M_B(p_\pi) = \int \frac{d^3p}{(2\pi)^3} \phi(\mathbf{p}) M_{\pi\pi}(\mathbf{p}_\pi, \mathbf{p}) = \int d^3r \psi(\mathbf{r}) M_{\pi\pi}(\mathbf{p}_\pi, \mathbf{r}) \quad (20)$$

by fourier transforming  $\phi(\mathbf{p})$  and  $M_{\pi\pi}(\mathbf{p}_\pi, \mathbf{p})$ . The angular integral  $d\Omega_\pi$  in Eq. (19) runs over the full solid angle of one of the pions due to wave function symmetrization [3].

The amplitude  $M_{\pi\pi}(\mathbf{p}_\pi, \mathbf{p})$  refers to  $K\bar{K}$  annihilation where the pions are on-shell with the magnitude of their common momentum fixed by total energy conservation at  $p_\pi = (\frac{1}{4}P_0^2 - m_\pi^2)^{1/2}$ ; the kaons remain off-shell as before.  $M_{\pi\pi}(\mathbf{p}_\pi, \mathbf{p})$  is then given by  $\hat{\Gamma}_i(\mathbf{p}_\pi, \mathbf{p}; P_0) + \hat{\Gamma}_i(-\mathbf{p}_\pi, \mathbf{p}; P_0)$  from Eq. (4) with  $g_i^2 C_i n_s = -\sqrt{3}g_{\pi K K^*}^2$  and  $M_i = M_{K^*}$ . The  $\mathbf{p}_\pi \rightarrow -\mathbf{p}_\pi$  crossed contribution comes about since the pions are identical bosons in the symmetrized space  $\times$  isospin basis [3]. Performing the fourier transform of this sum gives the transition operator in coordinate space as

$$M_{\pi\pi}(\mathbf{p}_\pi, \mathbf{r}) = -2\sqrt{3}g_{\pi K K^*}^2 e^{-i\mathbf{p}_\pi \cdot \mathbf{r}} \left\{ \delta^3(\mathbf{r}) + \left[ P_0^2 + 4p_\pi^2 - M_{K^*}^2 + 4i(\mathbf{p}_\pi \cdot \nabla) \right] \frac{e^{-M^* r}}{4\pi r} \right\} \quad (21)$$

after discarding the quartic terms of order  $\mathcal{O}(M_K^2/4M_{K^*}^2) \ll 1$ . The delta function contribution arises from the quadratic dependence on the momentum transfer  $\mathbf{q} = \mathbf{p} - \mathbf{p}_\pi$  in the numerator of Eq. (4) that introduces the Laplacian  $\nabla^2$  operating on the Yukawa-like potential in coordinate space produced by the  $K^*$  meson exchange. We insert this result into the second form of Eq. (20) with  $\psi(\mathbf{r}) = \psi(0)u(r)/r$  to find

$$M_B(p_\pi) = -8\pi\alpha_{\pi\pi}\psi(0)R(p_\pi) \quad (22)$$

where  $\alpha_{\pi\pi}$  is an effective coupling constant at zero kaon momentum

$$\alpha_{\pi\pi} = -\frac{\Gamma_i(\mathbf{p}_\pi, 0; P_0)}{4\pi} = \frac{1}{4}\sqrt{3}\alpha_s \left[ \frac{P_0^2 + p_\pi^2}{M_{K^*}^2 + p_\pi^2} \right] \approx 1.489 \quad (23)$$

for  $\alpha_s = 2.9$  and  $P_0 \approx 2M_K$ . This determines the annihilation cross section for free  $K\bar{K}$  pairs into two pions at low momentum as

$$\sigma_0 = \frac{\pi\alpha_{\pi\pi}^2 p_\pi}{M_K^2 p}. \quad (24)$$

The factor  $R$  is given by

$$R(p_\pi) = \left[ \frac{P_0^2 + p_\pi^2}{M_{K^*}^2 + p_\pi^2} \right]^{-1} \times \left[ 1 + (P_0^2 + 4p_\pi^2 - M_{K^*}^2) \left( \int_0^\infty dr u(r) j_0(p_\pi r) e^{-M_{K^*} r} \right) - 4p_\pi^2 \left( \int_0^\infty dr u(r) (1 + M_{K^*} r) \frac{j_1(p_\pi r)}{p_\pi r} e^{-M_{K^*} r} \right) \right] \quad (25)$$

The  $j_l(p_\pi r)$  are spherical Bessel functions. Then Eq. (19) reads

$$\Gamma_{\pi\pi} = \left( \frac{2\pi\alpha_{\pi\pi}^2 p_\pi}{M_K^2 M_K} \right) \psi^2(0) R^2(p_\pi) = (v_{rel}\sigma_0) \psi^2(0) R^2(p_\pi) \quad (26)$$

where  $v_{rel} = 2p/M_K$  is the relative c.m. velocity of either kaon and  $p_\pi = 0.959 M_K$  is now the pion momentum at threshold. For  $R = 1$ , Eq. (26) reduces to the familiar ‘‘wave function at contact’’ approximation for the decay width [2, 5, 26, 28] where only the probability per unit volume  $\psi^2(0)$  of finding the pair at the origin characterizes the bound state.

The isovector  $K\bar{K} \rightarrow \pi^0\eta$  decay width  $\Gamma_{\pi^0\eta}$  is given by a similar expression with the following replacements in Eqs. (24) to (26):  $p_\pi$  by  $p_{\pi\eta} = 0.658 M_K$ ,  $P_0^2$  by  $(E_\eta + \frac{1}{2}P_0)(E_{\pi^0} + \frac{1}{2}P_0)$ , and  $M_{K^*}^2$  by  $\hat{M}_{K^*}^2 = M_{K^*}^2 + (E_\eta - \frac{1}{2}P_0)(E_{\pi^0} - \frac{1}{2}P_0)$ . These modifications of the vertex in Eq. (4) reflect the revised total energy conservation condition,  $P_0 = E_{\pi^0} + E_\eta$  for an on-shell  $\pi^0\eta$  pair in the final state with energies  $E_{\pi^0}$  and  $E_\eta$  and common c.m. momentum  $p_{\pi\eta}$ . Then  $\alpha_{\pi\pi}$  is replaced by

$$\alpha_{\pi\eta} = \frac{1}{4}\sqrt{\frac{3}{2}}\alpha_s \left[ \frac{(E_\eta + \frac{1}{2}P_0)(E_{\pi^0} + \frac{1}{2}P_0) + p_{\pi\eta}^2}{\hat{M}_{K^*}^2 + p_{\pi\eta}^2} \right] \approx 1.079 \quad (27)$$

after removing the crossed contribution;  $\psi(0)$  now refers to the isovector channel.

In Eq. (26) both  $\psi(0)$  and  $R$  are functions of the binding energy;  $R$  in particular only differs significantly from unity when the ranges of the radial wave function  $u(r)$  and the amplitude  $M_{\pi\pi}(\mathbf{p}_\pi, \mathbf{r})$  under the integrals in Eq. (25) are commensurate. This is the case for the analogous  $M_{\gamma\gamma}(\mathbf{p}_\gamma, \mathbf{r})$  that describes two-photon decay [26]. However for the loosely bound  $K\bar{K}$  pairs in Tables I and II,  $u(r)$  has a typical range  $\sim M_K^{-1}$  that is about twice the range  $M_{K^*}^{-1}$  of the transition operator. Then only the short range behavior of  $u(r)$  is important for determining  $R$ . This behavior does not differ very much from the small  $r$  limit,  $u(r) = r$ , when both integrals have the common value  $(M_{K^*}^2 + p_\pi^2)^{-1}$ . This gives  $R = 1$ , thereby reproducing the wave function at contact approximation. The same result follows immediately from the momentum space representation of  $M_B(p_\pi)$  in the weak binding limit when  $\phi(\mathbf{p})$  has a much shorter range than the transition operator in momentum space. Then the integral evaluates approximately as  $M_{\pi\pi}(\mathbf{p}_\pi, 0)\psi(0)$  that leads directly back to Eq. (22) again with  $R = 1$ .

The calculated widths are listed in Table I. Since the cross section factors  $v_{rel}\sigma_I$  for free annihilation are fixed by the coupling constants  $\alpha_{\pi\pi}$ ,  $\alpha_{\pi\eta}$ , the values of the decay widths given by Eq. (26) and its  $I = 1$  counterpart are controlled by the real  $K\bar{K}$  potential that determines  $\psi(0)$  and  $R$  in each isospin channel. The cutoffs  $\Lambda$  have been fixed to reproduce a prescribed binding energy range. There are thus no free parameters. The predicted widths in Table I cover a range for  $\Gamma_{\pi\pi}$  that agrees quite well with experiment within the quoted error bars; the predicted values for  $\Gamma_{\pi^0\eta}$  are too small.

The actual values of  $R$  listed in Table II for  $I = 0$  increase only slightly with binding energy from 1.034 to 1.041 over the entire range of  $\epsilon_0$ . The behavior for  $I = 1$  is similar. Thus the main variation in width in Table I comes from the contact probability density  $\psi^2(0)$  which increases approximately like  $\sqrt{\epsilon_I}$ ; higher binding enhances the probability of contact at the origin. From a quark model perspective [1] this increased contact probability facilitates strange quark annihilation and exchange to produce the  $(K\bar{K})_0 \rightarrow \pi\pi$  and  $(K\bar{K})_1 \rightarrow \pi^0\eta$  decays respectively.

### Contributions from $s$ -channel scalar meson exchange

The calculations of mass and widths just presented for the  $K\bar{K}$  system ignore any  $s$ -channel contributions to the scattering amplitude  $\hat{\Gamma}(\mathbf{p}', \mathbf{p}; P_0)$  in Eq. (1). However,  $K\bar{K}$  can also interact and annihilate via scalar meson exchange in this channel. One expects such effects to be small because the exchanged particle is off-shell. As an example we estimate their order of magnitude contribution for the case of  $\sigma$  meson exchange, treated as a simple  $q\bar{q}$  state. Then the relevant interactions can be read off from the  $SU(3)$  linear sigma model (L $\sigma$ M) Lagrangian [12, 13, 29],

$$\mathcal{L}_{cubic} = g_{\sigma\pi\pi}\sigma(\vec{\pi} \cdot \vec{\pi}) + g_{\sigma K\bar{K}}\sigma\bar{K}K + \dots \quad (28)$$

The coupling constants are given by  $g_{\sigma\pi\pi} \approx M_\sigma^2/2f_\pi$ ,  $g_{\sigma K\bar{K}} \approx M_\sigma^2/2f_K$  in the (ideally mixed) chiral limit. The  $(f_\pi, f_K) \approx (92.2, 110)$  MeV with  $f_K/f_\pi \approx 1.19$  are the pion and kaon weak decay constants [11].

The relevant diagrams are shown in Fig. 3. Translating these diagrams one finds a  $s$ -channel contribution to the BS equation scattering amplitude coming from  $\sigma$  exchange as

$$\hat{\Gamma}_\sigma(\mathbf{p}', \mathbf{p}; P_0) = -(\sqrt{2}g_{\sigma K\bar{K}})^2\mathcal{D}_\sigma(P_0^2) \quad (29)$$

for off-shell kaons with c.m. four-momentum squared  $s = P_0^2$ , where  $\mathcal{D}_\sigma(s) = [s - M_\sigma^2 - \Sigma_\sigma(s)]^{-1}$  is the ‘‘dressed’’ scalar meson propagator [15] of mass  $M_\sigma$  and self-energy  $\Sigma_\sigma(s)$ .

The  $s$ -channel contribution to the additional binding energy and decay width for  $I = 0$  is then given in first order by

$$\epsilon_0^{(\sigma)} + \frac{i}{2}\Gamma_{\pi\pi}^{(\sigma)} = \frac{1}{4M_K^2} \int \int \frac{d^3p'}{(2\pi)^3} \frac{d^3p}{(2\pi)^3} \phi(\mathbf{p}') [\hat{\Gamma}_\sigma(\mathbf{p}', \mathbf{p}; P_0)] \phi(\mathbf{p}) = -\frac{g_{\sigma K\bar{K}}^2}{2M_K^2} \psi^2(0) \mathcal{D}_\sigma(P_0^2). \quad (30)$$

In particular,

$$\Gamma_{\pi\pi}^{(\sigma)} = \pi \frac{g_{\sigma K\bar{K}}^2}{M_K^2} \psi^2(0) \rho_\sigma(P_0^2), \quad \rho_\sigma(s) = -\frac{1}{\pi} \text{Im} \mathcal{D}_\sigma(s) \quad (31)$$

where  $\rho_\sigma(s)$  is the scalar spectral density associated with  $\mathcal{D}_\sigma(s)$ .

The self-energy  $\Sigma_\sigma(s)$  receives contributions at one-loop level from tadpole and seagull diagrams in addition to polarisation diagrams generated by Eq. (28), plus counter-terms. Of these, only the polarization loop involving  $\pi\pi$  for  $I = 0$  (or  $\pi\eta$  for  $I = 1$ ) has an imaginary part for strong decay at the relevant four-momentum transfer encountered in Eqs. (30) and (31). Cutting the loop in the standard way places both pions on-shell and gives the imaginary part

$$- \text{Im} \Sigma_\sigma(s) = \frac{3g_{\sigma\pi\pi}^2}{8\pi} \left(1 - \frac{4M_\pi^2}{s}\right)^{1/2} \theta(s - 4M_\pi^2) = M_\sigma \Gamma_\sigma(s), \quad (32)$$

The last equality defines an “off-shell” width  $\Gamma_\sigma(s)$  that coincides with the physical decay width for  $\sigma \rightarrow \pi\pi$  at  $s = M_\sigma^2$ . Evaluating  $\rho_\sigma(s)$  in Eq. (31) at  $s = P_0^2$ , one has

$$\Gamma_{\pi\pi}^{(\sigma)} = \frac{3p_\pi}{8\pi} \frac{\psi^2(0)}{M_K^3} \left\{ \frac{g_{\sigma\pi\pi}^2 g_{\sigma K\bar{K}}^2}{(P_0^2 - M_\sigma^2)^2 + (Im\Sigma_\sigma(P_0^2))^2} \right\} \quad (33)$$

after absorbing  $Re\Sigma_\sigma(s)$  into a redefinition of the  $\sigma$  mass  $M_\sigma^2 + (Re\Sigma_\sigma(P_0^2))^2 \rightarrow M_\sigma^2$ . The c.m. momentum  $p_\pi$  refers to outgoing pions from the  $K\bar{K} \rightarrow \pi\pi$  decay as before. The binding energy contribution  $\epsilon_0^{(\sigma)}$  follows from the real part of Eq. (30) as

$$\epsilon_0^{(\sigma)} = (P_0^2 - M_\sigma^2)[2Im\Sigma_\sigma(P_0^2)]^{-1}\Gamma_{\pi\pi}^{(\sigma)} < 0, \quad (34)$$

i.e. the contribution to the real potential from the  $s$ -channel is repulsive (less binding) for  $P_0 \geq M_\sigma$ .

We identify  $\sigma$  with the  $f_0(600)$  scalar meson and take its mass and decay half-width parameters as  $M_\sigma - \frac{i}{2}\Gamma_\sigma = [(541 \pm 39) - (252 \pm 42)i]$  MeV directly from experiment [30]. By inverting Eq. (32) for the  $\sigma \rightarrow \pi\pi$  width the coupling constant is determined as  $g_{\sigma\pi\pi} = 1.63 \pm 0.17$  GeV. Since this value is quite close to the chiral model estimate of  $g_{\sigma\pi\pi} = M_\sigma/2f_\pi \approx 1.48$  GeV, we assume that the L $\sigma$ M coupling constant ratio  $(g_{\sigma\pi\pi})/(g_{\sigma K\bar{K}}) = f_K/f_\pi \approx 1.19$ , also continues to hold to fix  $g_{\sigma K\bar{K}} = 1.37$  GeV. These parameters lead to  $I = 0$  contributions from the  $s$ -channel of

$$\epsilon_0^{(\sigma)} + \frac{i}{2}\Gamma_{\pi\pi}^{(\sigma)} = -8.92 + 3.93i, \quad -5.18 + 2.28i \quad \text{and} \quad -2.92 + 1.29i \text{ MeV} \quad (35)$$

respectively for cutoffs  $\Lambda = 415, 420$  and  $425$  MeV.

The exchange of other scalar mesons also has to be addressed. Since both  $f_0(980)$  and  $a_0(980)$  are depicted as  $K\bar{K}$  molecules in the Weinstein–Isgur picture used here, the next available set of scalars to consider would be the  $0^+$  states  $f_0(1370), K_0^*(1430), a_0(1450)$  and  $f_0(1500)$  with masses above 1.3 GeV. However a consistent theoretical description of these scalars is still under debate. If, as suggested in [12, 13, 29], one places them in the same  $q\bar{q}$  scalar nonet and implements a linear sigma model description, the decay widths of, for example,  $a_0(1450)$  into  $K\bar{K}$  and  $\pi^0\eta$  come out far too large. This is in part due to the large coupling constants generated by the model [13]. On the other hand if one *assumes* an interaction of the L $\sigma$ M form, but extracts the relevant coupling constants  $(g_{a_0\pi\eta}, g_{a_0K\bar{K}}) \approx (1.34, 0.95)$  GeV from the  $a_0(1450)$  branching ratios [11] into  $\pi^0\eta$  ( $\sim 8\%$ ) and  $K\bar{K}$  ( $\sim 7\%$ ), the  $I = 1$  contributions are given by

$$\epsilon_1^{(a_0)} + \frac{i}{2}\Gamma_{\pi^0\eta}^{(a_0)} = 2.16 + 0.085i, \quad 1.15 + 0.045i \quad \text{and} \quad 0.59 + 0.023i \text{ MeV} \quad (36)$$

for  $s$ -channel  $a_0(1450)$  exchange. We omit the calculational details.

None of these contributions introduce any significant corrections into the  $t$ -channel values of Table I. This is because the scalar spectral density is sampled at  $s \approx 4M_K^2$  that pushes the exchanged meson significantly off its mass-shell to weaken the  $s$ -channel  $K\bar{K}$  interaction accordingly. In addition, the small partial decay width  $\sim 20$  MeV for  $a_0(1450) \rightarrow \pi^0\eta$  relative to  $\sigma \rightarrow \pi\pi$  serves to suppress the  $I = 1$  contribution even further.

In closing this section we remark that the interaction vertices described by the effective Lagrangian involving only meson degrees of freedom can also be visualised at the constituent quark level. For instance the vertex  $K^+ + \bar{K}^{0*} \rightarrow \pi^+$ , that contributes to  $K^+K^- \rightarrow \pi^+\pi^-$  in Fig. 2 translates schematically into  $[(u\bar{s})(s\bar{d})] \rightarrow [u\bar{d}]$ , the strange quarks  $s\bar{s}$  having annihilated (via some unspecified gluon exchange interaction) leaving behind the  $u$  and  $\bar{d}$  quarks.

Moving beyond the effective meson theory model then, this suggests that in principle the final two-meson decay channels can for example also be reached via another route involving “constituent gluons” in intermediate states that give rise to hybrid meson structures  $[q\bar{q}g]$  (see [31] for a comprehensive review). Hybrids are generally expected [32, 33] to be heavier than 1.7–1.9 GeV, thus lifting the threshold of such intermediate states above 2 GeV and making them less important than the intermediate meson states which we have taken into account in the present context. Moreover, the hybrids’ predicted decay properties (for example no decays into two pseudoscalar mesons, at least according to the gluon flux-tube model [34] of their structure) can only further reduce their impact here. Further discussion of such contributions lies outside the scope of this article. We refer to the recent literature [31, 32, 33, 34] for more details.

#### IV. $K\bar{K}$ SCATTERING

It is straightforward to show that the standard effective range expansion [35] for the  $K\bar{K}$  scattering phase shift  $\delta_I(k)$  at c.m. momentum  $k = \sqrt{M_K E}$ ,

$$k \cot \delta_I(k) = -\frac{1}{a_I} + \frac{1}{2}r_I k^2 + \dots \quad (37)$$



continues to hold for the modified radial equation (14) in terms of the scattering length and effective range  $a_I$  and  $r_I$ .

In the presence of annihilation both parameters pick up imaginary contributions. In particular, in the limit  $k \rightarrow 0$ , the imaginary part of the  $I = 0$  scattering length  $a_0$  is related to the  $K\bar{K} \rightarrow \pi\pi$  annihilation cross section  $\tilde{\sigma}_0$  by

$$\begin{aligned} -\text{Im}(a_0) &= \frac{k}{4\pi}\tilde{\sigma}_0 \approx \frac{k}{4\pi}|f(0)|^{-2}\sigma_0 = |f(0)|^{-2}\xi_0^{-1} \\ \xi_0^{-1} &= \frac{k}{4\pi}\sigma_0 = \frac{\alpha_{\pi\pi}^2 p_\pi}{4M_K M_K} = (1.881M_K)^{-1}. \end{aligned} \quad (38)$$

The first step is exact. The next step follows after noting that  $\tilde{\sigma}_0$  is related to the free annihilation cross section  $\sigma_0$  of Eq. (24) by  $\tilde{\sigma}_0 \approx |f(0)|^{-2}\sigma_0$  to a good approximation [36]. Here  $f(k)$  is the Jost function [36, 37] that determines the scattering matrix  $S(k) = f(k)/f(-k)$ . The value  $|f(0)|^{-2}$  at  $k = 0$  is the enhancement factor [36] that gives the ratio of the probability of finding an interacting kaon pair at the origin to that when there is no interaction between them.

If one parametrizes the Jost function  $f(k) = |f(k)| \exp[i\delta_I(k)]$  as

$$f(k) = \frac{k - ia}{k - ib} \quad (39)$$

the effective range expansion becomes exact [37], and scattering length and effective range are given in terms of the parameters  $(a, b)$ . Considering  $I = 0$  again, one gets

$$a_0 = -(b - a)/ba, \quad r_0 = 2/(b - a). \quad (40)$$

Since the isoscalar channel supports a single  $s$ -wave bound state at complex binding energy  $\tilde{\epsilon}_0 = \epsilon_0 + \frac{i}{2}\Gamma_{\pi\pi}$  one knows that the function  $f(k)$  must have a zero [37] in the lower half of the complex  $k$  plane at  $k = ia = -i\sqrt{M_K\tilde{\epsilon}_0}$  which determines  $a$ . Combining Eqs. (38) and (40) one then finds  $b = \sqrt{\xi_0\text{Im}(-a)}$  for  $b$  real. An identical procedure suffices for determining  $(a, b)$  in the isovector channel.

The scattering parameters for both channels are then given by Eq. (40). Taking the relevant values of  $\tilde{\epsilon}_0$  and  $\tilde{\epsilon}_1$  from Table I for  $\Lambda = 420$  MeV, one calculates that

$$\begin{aligned} a_0 &= 4.926 - 2.235i, & r_0 &= 2.550 - 0.525i \\ a_1 &= 8.246 - 2.576i, & r_1 &= 2.971 - 0.242i \end{aligned} \quad (41)$$

in units of  $M_K^{-1}$ .

Apart from one pioneering experimental attempt to determine the isoscalar scattering length by Wetzell *et al.* [38] who find  $a_0 = [(3.13 \pm 0.30) - (0.67 \pm 0.07)i]M_K^{-1}$ , and a subsequent analysis of later  $\pi\pi$  data that infers [39]  $a_0 = (4.36 - 1.49i)M_K^{-1}$ , there are as yet no other direct  $K\bar{K}$  measurements with which to compare the estimates in Eq. (41). However, to the extent that only coupling between the  $\pi\pi$  and  $K\bar{K}$  channels is important, two channel unitarity shows [40] that the  $\pi\pi$  and  $K\bar{K}$  isoscalar inelasticities  $\eta_0(\pi\pi) = \eta_0(K\bar{K}) = |S_0(k)|$  are equal at their common total c.m. energy  $P_0 = 2\sqrt{p^2 + M_\pi^2} = 2\sqrt{k^2 + M_K^2}$  where  $p$  and  $k$  are the pion and kaon momenta. In Fig. 4 we compare  $\eta_0(\pi\pi)$  as calculated from  $S_0(k) = \exp[2i\delta_0(k)]$  in the effective range approximation, Eq. (37), using the isoscalar parameters given above, with the inelasticities extracted from  $\pi\pi$  scattering in Ref. [41]. The result using the isoscalar scattering parameters  $a_0 = (4.281 - 2.398i)M_K^{-1}$ ,  $r_0 = (1.169 - 0.178i)M_K^{-1}$  obtained from the local potential in [5] is also given for comparison. A recent  $K$ -matrix fit based on a combination of various data sets is also shown, see [42] and further references cited therein. Given the very wide error bars on the data it is difficult to draw definitive conclusions beyond remarking that the model calculations do reproduce the correct trend and order of magnitude of the  $\pi\pi$  inelasticity, albeit somewhat too low.

## V. KAONIUM

We next summarize the results obtained for the energy shifts and decay widths for the  $K^+K^-$  (kaonium) atom in the context of the present calculations. The properties of this system have already been discussed in detail in [5] for local potentials.

Pure Coulomb interactions bind kaonium at  $-\frac{1}{2}\alpha^2\mu = -6.576$  keV in the lowest  $1s$  state where  $\psi_{1s}(r) = \pi^{-1/2}(\mu\alpha)^{3/2}\exp(-\mu\alpha r)$ ;  $\mu = \frac{1}{2}M_{K^\pm}$  is the reduced mass with  $M_{K^\pm} \approx 494$  MeV, and  $\alpha \approx 1/137$  the fine structure constant. The kaonium  $\rightarrow \pi\pi + \pi^0\eta$  decay width follows from Eq. (26) after replacing  $\sigma_0$  by the total  $K^+K^-$

annihilation cross section  $\sigma_p = (\sigma_0 + \sigma_1)/2$  and  $\psi(0)$  by  $\psi_{1s}(0)$ . While  $R$  can be calculated in closed form for the  $1s$  Coulomb ground state of kaonium,

$$R_{1s}(p_\pi) = \left[ \frac{P_0^2 + p_\pi^2}{M_{K^*}^2 + p_\pi^2} \right]^{-1} \left[ \frac{P_0^2 + p_\pi^2 - \mu\alpha(2M_{K^*} + 3\mu\alpha)}{(M_{K^*} + \mu\alpha)^2 + p_\pi^2} + 4 \frac{\mu\alpha}{p_\pi} \cot^{-1} \left( \frac{M_{K^*} + \mu\alpha}{p_\pi} \right) \right] \quad (42)$$

this factor differs but little from unity,  $R_{1s}(p_\pi) = 1.0016$ ; the corresponding expression for  $I = 1$  gives  $R_{1s}(p_{\pi\eta}) = 1.0013$ . This is to be expected. The Bohr radius of kaonium,  $1/\mu\alpha = 109$  fm, is about 500 times the transition amplitude range of  $M_{K^*}^{-1} \sim 0.2$  fm. Hence the wave function at contact is a very reliable approximation in this case too and yields a total  $1s$  decay width of [51]

$$\Gamma_{1s} = \Gamma_{\pi\pi} + \Gamma_{\pi^0\eta} = \frac{1}{8}(\alpha_{\pi\pi}^2 p_\pi + \alpha_{\pi^0\eta}^2 p_{\pi\eta})\alpha^3 = (51.3 + 18.4) \text{ eV} = 69.7 \text{ eV}, \quad (43)$$

or a lifetime of  $\sim 10^{-17}$ s.

The effect of strong plus Coulomb interactions on the kaonium spectrum can be included in the standard way [35] by equating the logarithmic derivative of the asymptotic form  $u_p(r) \sim 1 - \alpha_p r$  of the zero energy  $K^+K^-$  scattering wave function outside the strong interaction zone with that of a pure incoming Coulomb wave function;  $\alpha_p$  is given below. Physically this suggests that the binding of kaonium is still essentially provided by the long range Coulomb attraction.

For bound states the Coulomb wave function is proportional to the Whittaker function [43]  $f_c^{(-)}(k, r) \sim W_{i\eta, 1/2}(2ikr)$  at complex wave number  $k_\lambda = -i\lambda\mu\alpha$  that describes a decaying wave at  $r \rightarrow \infty$ . Here  $\lambda$  is a yet to be determined eigenvalue that gives the binding energies and total decay widths  $E_\lambda - \frac{1}{2}i\Gamma_\lambda = -\frac{1}{2}\lambda^2\mu\alpha^2$  of the mesonic atom under the combined influence of strong and Coulomb interactions;  $i\eta = \mu\alpha/ik_\lambda = 1/\lambda$  is the Coulomb parameter for attractive interactions. The matching condition at the Bethe ‘‘Coulomb joining radius’’ [35]  $d$  say, is then equivalent to the Kudryavtsev–Popov equation [44] for the complex eigenvalues  $\lambda$  that takes the simple form [5]

$$(\alpha_p)_c = 2\mu\alpha \left[ \psi(1 - 1/\lambda) + \frac{1}{2}\lambda + \ln \lambda + \gamma \right] \quad (44)$$

for kaonium in the limit  $\mu\alpha d \ll 1$ , where  $\psi$  is the digamma function [45] and  $\gamma = 0.5771 \dots$  is Euler’s constant. The  $(\alpha_p)_c$  on the left is the Coulomb corrected  $K^+K^-$  inverse scattering length [35],

$$(\alpha_p)_c = \alpha_p - 2\mu\alpha[\ln(2\mu\alpha d) + \gamma]. \quad (45)$$

Here  $\alpha_p = 1/a_p$  is the inverse of the  $K^+K^-$  strong scattering length  $a_p = (a_0 + a_1)/2$  without Coulomb corrections if the isospin-breaking arising from the kaon mass difference  $\Delta = M_{K^0} - M_{K^\pm} \approx 4$  MeV [11] is ignored. If not, the  $K^+K^- \rightarrow K^0\bar{K}^0$  charge exchange channel is closed, and [46]

$$\alpha_p = \left( \frac{1 - k_0 a_p}{a_p - k_0 a_0 a_1} \right), \quad k_0 = \sqrt{2M_{K^0}\Delta}. \quad (46)$$

We take the scattering lengths of good isospin from Eq. (41), and calculate the Bethe joining radius as  $d = 1.636M_K^{-1}$  from the regular zero energy scattering solution of Eq. (14). Then  $\alpha_p = (6.873 - 3.387i)^{-1}M_K$  and  $(\alpha_p)_c = (5.948 - 2.364i)^{-1}M_K$ . Inserting this information on the left hand side of Eq. (44) one finds  $\lambda_{1s} = 0.9579 + 0.0161i$ , or

$$E_{1s} - \frac{i}{2}\Gamma_{1s} = (-6.027 - 0.205i) \text{ keV} \quad (47)$$

for the lowest state. Repeating the exercise for the remaining two values of the cutoff, the results for the energy shifts and decay widths for kaonium ground state can be summarized as follows,

$$\Delta E_{1s} - \frac{i}{2}\Gamma_{1s} = (0.549_{-0.106}^{+0.059} - 0.205_{-0.079}^{+0.100}i) \text{ keV}, \quad \Lambda = 420 \pm 5 \text{ MeV} \quad (48)$$

that illustrates the sensitivity to the choice of  $\Lambda$ . The corresponding lifetimes read  $\tau = 1.6_{+1.00}^{-0.5} \times 10^{-18}$ s.

Thus for  $\Lambda = 420$  MeV, apart from causing a repulsive level shift of  $\Delta E_{1s} = 0.549$  keV in the ground state energy of Coulombic kaonium, the strong interaction also enhances the decay width considerably to  $\Gamma_{1s} = 0.410$  keV over that calculated in Eq. (43). There is thus strong mixing between the pure Coulomb state and the  $f_0(980)$  molecular ground state that produces a significant increase in decay width (and energy shift of the same order) that shortens

the lifetime of the kaonium ground state to  $\sim 2 \times 10^{-18}$ s. These results are in line with previous estimates based on a local potential description [5].

The strong mixing feature  $\Gamma_{1s} \simeq \Delta E_{1s}$  persists for the excited states of kaonium as well. This is illustrated for  $\Lambda = 420$  MeV in Fig. 5 which shows the decay width versus the energy shift for the kaonium spectrum. The ratio is seen to remain remarkably constant over three orders of change in magnitude in these quantities as one moves through the Balmer spectrum of kaonium. This can be understood from the Deser *et al.* [47] perturbative solution of Eq. (44) that is obtained by expanding the roots  $\lambda^{-1}$  in powers of the corrected scattering length combination  $\mu\alpha(a_p)_c = \mu\alpha(\alpha_p)_c^{-1}$  around their pure Coulomb field values at  $\lambda_n^{-1} = n = 1, 2, 3, \dots$ . Then

$$\Delta E_{ns} - \frac{i}{2}\Gamma_{ns} = \frac{2\mu^2\alpha^3}{n^3}(a_p)_c \left[ 1 + 2\mu\alpha(a_p)_c \left( \psi(n) - \psi(1) + \frac{1}{2n} - \ln n \right) + \dots \right] \quad (49)$$

that has a very similar structure to the analogous chiral perturbation theory result for kaonic hydrogen [48]. Working to lowest order, one retrieves the Deser formula

$$\Delta E_{ns} - \frac{i}{2}\Gamma_{ns} \approx \frac{2\mu^2\alpha^3}{n^3}(a_p)_c = (0.575 - 0.228i) \text{ keV}, \quad n = 1, \quad (50)$$

which gives  $n = 1$  shift and width values that are 5 and 11% too large in comparison with Eq. (48). The relation  $\Gamma_{ns} = -2Im(a_p)_c/Re(a_p)_c\Delta E_{ns} = 0.79\Delta E_{ns}$  that follows from the latter result gives the straight line in Fig. 5.

The underlying reason for the mixing can be qualitatively understood by temporarily ignoring annihilation so that  $\alpha_p$  is real and positive. Then one sees from the asymptotic form of  $u_p(r)$  that the kaonium ground and excited state wave functions of Fig. 5 all develop a common additional node at  $r = 1/\alpha_p$  that renders them orthogonal to the ground state wave function of the bound  $K\bar{K}$  pair. They are consequently all excited states in the combined strong plus Coulomb potentials, that suffer level repulsion with the kaon-antikaon ground state.

## VI. SUMMARY AND CONCLUSIONS

It is shown that the  $K\bar{K}$  momentum-dependent interaction due to vector meson exchange can be incorporated without further approximation into a non-relativistic Bethe-Salpeter wave equation in coordinate space containing, in addition to a local potential, a spatially dependent effective kaon mass embedded in a fully symmetrized kinetic energy operator.

A numerical analysis of the possible bound and scattering states of this modified equation is presented as a model for the properties of a molecular kaon-antikaon description of the light scalar mesons  $f_0(980)$  and  $a_0(980)$ . We show that for a restricted range of cutoffs  $\Lambda$ , the only adjustable parameter in the calculations, one obtains bound state masses for both scalar mesons in reasonable accord with experiment. The accompanying  $\pi\pi$  and  $\pi^0\eta$  decay widths exhibit a substantial variability with  $\Lambda$  since they are sensitive to the contact probability density as determined by the ground state eigenfunction. The results can be displayed in round numbers as follows

$$M_0 - \frac{i}{2}\Gamma_{\pi\pi} = [(988 \text{ to } 971) - \frac{i}{2}(36 \text{ to } 108)] \text{ MeV}; \quad M_1 - \frac{i}{2}\Gamma_{\pi^0\eta} = [(989 \text{ to } 976) - \frac{i}{2}(7 \text{ to } 27)] \text{ MeV} \quad (51)$$

as the cutoff  $\Lambda$  increases from 415 to 425 MeV. The predicted range for  $\Gamma_{\pi\pi}$  overlaps nicely with the experimental spread of values (40 – 100) MeV; the decay widths  $\Gamma_{\pi^0\eta}$  for molecular  $a_0(980)$  are too small. We also demonstrated at the end of Section III that the associated  $s$ -channel contributions to the binding energy and decay widths in both isospin channels are unimportant.

These calculations treat the decay vertices as point-like. Introducing a form factor like that of Eq. (6) replaces  $R \sim 1$  by  $R_\Lambda \sim 0.34$  in the transition amplitude of Eq. (22) if we assume the same cutoffs again as used for the potentials, see Appendix Eq. (A.7). Then one obtains an order of magnitude reduction in widths down to  $\Gamma_{\pi\pi} \simeq (4 - 12)$  and  $\Gamma_{\pi^0\eta} \simeq (1 - 3)$  MeV from those given in Eq. (51). This agrees qualitatively with the calculations in [49] that also find small decay widths of this order from a numerical study of the relativistic Bethe-Salpeter integral equation for the  $K\bar{K}$  system when form factors are included. They in addition find that bound states only occur for cutoffs  $\Lambda$  lying in a series of narrow windows similar to the one illustrated in Fig. 1 for the non-relativistic case.

The low energy parameters for  $K\bar{K}$  scattering in the presence of annihilation have also been calculated in both isospin channels. In particular this information allows one to construct the  $K\bar{K}$  isoscalar inelasticity as a function of the total energy in order to compare with the measured  $\pi\pi$  inelasticity which it equals in the two-channel problem considered here. The qualitative agreement with experiment is satisfactory.

Finally, the effect of strong interactions on the binding energy and decay of the  $K^+K^-$  mesonic atom are briefly discussed in the context of momentum-dependent potential model. The energy shifts and decay widths so obtained

are again not very different from those using the local potential approximation, and give a lifetime of  $\sim 2 \times 10^{-18}$ s for kaonium.

Overall, one can conclude that both the local and non-local potential description for the interaction of a  $K\bar{K}$  pair lead to very similar results that are only dependent on the cutoff required in the form factor of the potential for obtaining bound states. However the width predictions of either of these, or other [49], calculations remain ambiguous, depending as they do on whether the vertices in the transition amplitudes are regarded as point-like or extended. The calculation from first principles of such hadronic size effects lies beyond the scope of the present work. Without a better understanding of this latter aspect, one cannot decide on the basis of width predictions alone between the molecular versus elementary particle interpretations of the dynamics governing the structure of the light scalar mesons. What has been shown here, however, is that the molecular model for  $f_0(980)$  and  $a_0(980)$  with either local or non-local meson exchange interaction potentials does give reasonable mass and width predictions for the isoscalar channel in particular, assuming point-like vertices in the decay amplitudes. In this regard, observation of the energy shift and decay width in kaonium, which in combination directly probe the strong  $K^+K^-$  scattering length, would be a particularly important source of experimental information for further progress towards a better understanding of these interesting systems.

## VII. ACKNOWLEDGMENTS

This research was supported by a grant from the Ernest Oppenheimer Memorial Trust, which is gratefully acknowledged. I would also like to thank David Bugg for bringing Ref. [30] to my attention, and Veljko Dmitrasinović for constructive correspondence.

## APPENDIX

### Decay widths with form factors

In order to include a form factor in the transition operator  $M_{\pi\pi}(\mathbf{p}_\pi, \mathbf{r})$  of Eq. (21) we replace the pure Yukawa potential in that equation by  $U_i(r)$  from Eq. (8) with  $M_i = M_{K^*}$  and  $c_i = M_{K^*}/\sqrt{2}\Lambda$ . Then the revised transition amplitude splits into two parts,

$$M_{\Lambda, \pi\pi}(\mathbf{p}_\pi, \mathbf{r}) = -2\sqrt{3}g_{\pi K K^*}^2 e^{-i\mathbf{p}_\pi \cdot \mathbf{r}} \times \left[ \delta_\Lambda^3(\mathbf{r}) - \{P_0^2 + 4p_\pi^2 + 4i\mathbf{p}_\pi \cdot \nabla\}U_\Lambda(r) + \{P_0^2 + 4p_\pi^2 - M_{K^*}^2 + 4i\mathbf{p}_\pi \cdot \nabla\} \frac{e^{-M_{K^*}r}}{4\pi r} \right] \quad (\text{A.1})$$

after using

$$-\nabla^2 U_i(r) = -M_{K^*}^2 \frac{e^{-M_{K^*}r}}{4\pi r} + \delta_\Lambda^3(\mathbf{r}) \quad (\text{A.2})$$

where

$$U_\Lambda(r) = \frac{e^{-\sqrt{2}\Lambda r}}{4\pi r} \sum_{n=0}^3 C_n^{(0)} (\sqrt{2}\Lambda r)^n \quad (\text{A.3})$$

and

$$\delta_\Lambda^3(\mathbf{r}) = (\sqrt{2}\Lambda)^2 \frac{e^{-\sqrt{2}\Lambda r}}{4\pi r} \sum_{n=0}^3 C_n^{(2)} (\sqrt{2}\Lambda r)^n. \quad (\text{A.4})$$

The coefficients  $C_n^{(2)}$  are linear combinations of the  $C_n^{(0)}$ :  $C_0^{(2)} = (C_0^{(0)} - 2C_1^{(0)} + 2C_2^{(0)})$ ,  $C_1^{(2)} = (C_1^{(0)} - 4C_2^{(0)} + 6C_3^{(0)})$ ,  $C_2^{(2)} = (C_2^{(0)} - 6C_3^{(0)})$  and  $C_3^{(2)} = C_3^{(0)}$ . Since  $\delta_\Lambda^3(\mathbf{r}) \rightarrow 0$  or  $\infty$  depending on the order of the limits  $\Lambda \rightarrow \infty$ ,  $r \rightarrow 0$ , while

$$\int d^3r \delta_\Lambda^3(\mathbf{r}) = \sum_{n=0}^3 C_n^{(2)} \Gamma(n+2) = 1 \quad (\text{A.5})$$

independent of  $\Lambda$ , the function defined by Eq. (A.4) is a representation of a spread-out delta function for finite  $\Lambda$ . Clearly  $M_{\Lambda, \pi\pi}(\mathbf{p}_\pi, \mathbf{r})$  reverts back to  $M_{\pi\pi}(\mathbf{p}_\pi, \mathbf{r})$  when  $\Lambda \rightarrow \infty$ . For  $\Lambda \neq \infty$  Eq. (A.1) shows that the factor  $R(p_\pi)$  in the bound to free transition amplitude of Eq. (22) is replaced by

$$\begin{aligned}
R_\Lambda(p_\pi) = & \left[ \frac{P_0^2 + p_\pi^2}{M_{K^*}^2 + p_\pi^2} \right]^{-1} \left[ \left( (\sqrt{2}\Lambda)^2 \sum_{n=0}^3 C_n^{(2)} - (P_0^2 + 4p_\pi^2) \sum_{n=0}^3 C_n^{(0)} \right) \left( \int_0^\infty dr u(r) j_0(p_\pi r) (\sqrt{2}\Lambda r)^n e^{-\sqrt{2}\Lambda r} \right) \right. \\
& + 4p_\pi^2 \left( \int_0^\infty dr u(r) [(1 + \sqrt{2}\Lambda r) + \sum_{n=2}^4 C_n^{(1)} (\sqrt{2}\Lambda r)^n] \frac{j_1(p_\pi r)}{p_\pi r} e^{-\sqrt{2}\Lambda r} \right) \\
& \left. + (P_0^2 + 4p_\pi^2 - M_{K^*}^2) \left( \int_0^\infty dr u(r) j_0(p_\pi r) e^{-M_{K^*} r} \right) - 4p_\pi^2 \left( \int_0^\infty dr u(r) (1 + M_{K^*} r) \frac{j_1(p_\pi r)}{p_\pi r} e^{-M_{K^*} r} \right) \right]
\end{aligned} \tag{A.6}$$

with  $C_2^{(1)} = (C_1^{(0)} - C_2^{(0)})$ ,  $C_3^{(1)} = (C_2^{(0)} - 2C_3^{(0)})$  and  $C_4^{(1)} = C_3^{(0)}$ . Setting  $u(r) \rightarrow r$  again that characterizes the weak binding limit one confirms by direct calculation that now

$$R_\Lambda(p_\pi) = \left( \frac{2\Lambda^2 - M_{K^*}^2}{2\Lambda^2 + p_\pi^2} \right)^4 = F_i^2(p_\pi^2) \tag{A.7}$$

instead of unity, where  $F_i(p_\pi^2)$  is the form factor given by Eq. (6) evaluated at  $M_i = M_{K^*}$  and  $\mathbf{q}^2 = p_\pi^2$ . For  $\Lambda = 420$  MeV the actual values are  $R_\Lambda = 0.39$  versus  $F_i^2 = 0.34$  so the wave function at contact approximation continues to hold as well. Thus, depending on the value of the cutoff chosen, including a form factor in the transition amplitudes can reduce both the  $\pi\pi$  and  $\pi^0\eta$  widths in Table I by an order of magnitude.

- 
- [1] J. Weinstein and N. Isgur, Phys. Rev. Lett. **48** 659 (1982); Phys. Rev. D **27**, 588 (1983); D **41** 2236 (1990).  
[2] T. Barnes, Phys. Lett. **165 B** 434 (1985).  
[3] D. Lohse, J. W. Durso, K. Holinde and J. Speth, Nucl. Phys. **A516**, 513 (1990); G. Janßen, B. C. Pearce, K. Holinde and J. Speth, Phys. Rev. D **52**, 2690 (1995).  
[4] J. A. Oller, Nucl. Phys. **A714**, 161 (2003).  
[5] S. Krewald, R. H. Lemmer and F. P. Sassen, Phys. Rev. D **69**, 016003 (2004).  
[6] T. Branz, T. Gutsche and V.E. Lyubovitchij, Eur. Phys. J. A **37**, 303 (2008).  
[7] L. Montanet, Nucl. Phys. B (Proc. Suppl.) **86** 381 (2000); V.V. Anisovich *et al.*, Phys. Lett. **B480** 19 (2000).  
[8] N. N. Achasov and V. N. Ivanchenko, Nucl. Phys. **B315** 465 (1989).  
[9] R. Kokoski and N. Isgur, Phys. Rev. D **35** 907 (1987).  
[10] R. H. Lemmer and R. Tegen, Phys. Rev. C **66** 065202 (2002).  
[11] C. Amsler *et al.*, (Particle Data Group), Phys. Lett. **B667**, 1 (2008).  
[12] M. D. Scadron, G. Rupp, F.Kleefeld, and E. van Beveren, Phys. Rev. D **69**, 014010 (2004); Erratum-ibid. D **69**, 059901 (2004).  
[13] V. Dmitrasinović, Phys. Rev. C **53**, 1383 (1996).  
[14] M. R. Pennington, Prog. Theor. Phys. Suppl. **168**, 143 (2007) [arXiv:hep-ph/0703256v1].  
[15] See, for example, L. D. Landau and E. M. Lifshitz, *Relativistic quantum theory*, Course of Theoretical Physics Vol. 4 (Pergamon, Oxford, 1974).  
[16] W.L. Lucha, K. Maung Maung and F. F. Schöberl, Phys. Rev. D **64**, 036007 (2001).  
[17] Y.-J. Zhang, H.-C. Chiang, P.-N. Shen and B.-S. Zou, Phys. Rev. D **74**, 014013 (2006).  
[18] J. J. de Swart, Rev. Mod. Phys. **35** 916 (1963).  
[19] K. Kawarabayashi and M. Susuki, Phys. Rev. Lett, **16**, 255 (1966); X. Riazuddin and X. Fayyazuddin, Phys. Rev. **147**, 1071 (1966).  
[20] F. Q. Wu, B. S. Zou, L. Li and D. V. Bugg, Nucl. Phys. **A735**, 111 (2004).  
[21] W. E. Frahn and R. H. Lemmer, Nuovo. Cim. **5**, 523, 1564 (1957); *ibid* **6**, 1221 (1957).  
[22] For recent reviews and applications see P. Fröbrich and R. Lipperheide, *Theory of Nuclear Reactions*, (Oxford: Clarendon Press, New York: Oxford University Press, 1996); A. Lovell and K. Amos, Phys. Rev. C **62**, 064614 (2000).  
[23] Fermilab E791 Collaboration, E. M. Aitala *et al.*, Phys. Rev. Lett. **86** 765 (2001).  
[24] KLOE Collaboration, A. Aloisio, *et al.*, Phys. Lett. **B536**, 209 (2002).  
[25] OBELIX Collaboration, M. Bargiotti, *et al.*, Eur. Phys. J. C **26**, 371 (2003).  
[26] R. H. Lemmer, Phys. Lett. **B650**, 152 (2007).  
[27] C. Hanhart, Yu. S. Kalashnikova, A. E. Kudryavtsev, and A. V. Nefediev, Phys. Rev. D **75**, 074015 (2007).  
[28] J. A. Wheeler, Ann. NY Acad. Sci. **48** 219 (1946); M. A. Stroschio, Phys. Rep. C **22**, 215 (1975).  
[29] J. Schechter and Y. Ueda, Phys. Rev. D **3**, 2874 (1971).

- [30] BES Collaboration, M. Ablikim, *et al.*, Phys. Lett. **B598**, 149 (2004).
- [31] E. Klempt and A. Zaitsev, Phys. Rep. **454**, 1 (2007).
- [32] N. Isgur and J. E. Paton, Phys. Rev. D **31**, 2910 (1985).
- [33] I. J. General, S. R. Cotanch, and F. J. Llanes–Estrada, Eur. Phys. J. **C 51**, 347 (2007).
- [34] F. E. Close and P. R. Page, Phys. Rev. D **52**, 1706 (1995).
- [35] H. A. Bethe, Phys. Rev. **76**, 38 (1949); J. D. Jackson and J. M. Blatt, Rev. Mod. Phys. **22**, 77 (1950).
- [36] See, for example, M. L. Goldberger and K. M. Watson, *Collision Theory*, (John Wiley and Sons, New York, 1964), chapter 9.
- [37] V. Bargmann, Rev. Mod. Phys. **21**, 488 (1949); R. G. Newton, J. Math. Phys. **1**, 319 (1960).
- [38] W. W. Wetzel *et al.*, Nucl. Phys. **B115**, 208 (1976).
- [39] R. Kamiński and L. Leśniak, Phys. Rev. C **51**, 2264 (1995).
- [40] J. L. Petersen, Phys. Rep. **2C**, 155 (1971).
- [41] B. Hyams *et al.*, Nucl. Phys. **B64**, 134 (1973).
- [42] R. Kamiński, J. R. Pelaez, and F. J. Ynduráin, Phys. Rev. D **74**, 014001 (2006); Phys. Rev. D **74**, 079903(E) (2006).
- [43] See, for example, R. G. Newton, *Scattering Theory of Waves and Particles* (McGraw–Hill, New York, 1966).
- [44] A. E. Kudryavtsev and V. S. Popov, JETP Lett. **29**, 280 (1979); V. S. Popov, A. E. Kudryavtsev, and V. D. Mur, Sov. Phys. JETP **50**, 865 (1979).
- [45] M. Abramowitz and I. A. Stegun, Editors, *Handbook of Mathematical Functions* (Dover Publications, Inc., New York, 1965).
- [46] A. D. Martin and G. G. Ross, Nucl. Phys. **B16**, 479 (1970).
- [47] S. Deser, M. L. Goldberger, K. Baumann, and W. Thirring, Phys. Rev. **96**, 774 (1954).
- [48] Ulf–G. Meißner, U. Raha and A. Rusetsky, Eur. Phys. J. **C 35**, 349 (2004).
- [49] X–H. Guo and X–H. Wu, Phys. Rev. D **76**, 056004 (2007).
- [50] Without this restriction a physical problem arises because Eqs. (12) or (14) then develop a regular singular point at  $r = r_s > 0$  where  $\gamma(r_s) = 0$ . There is no difficulty in solving the resulting differential equation and continuing the solution through  $r_s$ , where  $u(r_s)$  is finite but has an infinite first derivative there. However such solutions lead to a probability current density that diverges at the singularity.
- [51] The analogous expressions quoted in [17] for  $M_B(p_\pi)$  and its isovector counterpart do not take into account the delta function singularity in the transition operator of Eq. (21) in either channel, and neglect crossing in the  $\pi\pi$  channel. As a result the kaonium decay widths given there underestimate those in Eqs. (43) and (48) by an order of magnitude.

TABLE I: Calculated values (in MeV) of the isoscalar ( $\epsilon_0$ ) and isovector ( $\epsilon_1$ ) binding energies and resulting masses  $M_I = 2M_K - \epsilon_I$  and annihilation widths for  $f_0(980)$  and  $a_0(980)$  for varying cutoff  $\Lambda$  as given by the non-local meson exchange potential model. Theoretical and experimental values from various sources have also been listed.

$\Lambda$	$\epsilon_0$	$M_0 - \frac{i}{2}\Gamma_{\pi\pi}$	$\epsilon_1$	$M_1 - \frac{i}{2}\Gamma_{\pi^0\eta}$
415	21.3	$971 - 54 i$	15.5	$976 - 13.7 i$
420	10.6	$981 - 33 i$	7.55	$984 - 7.30 i$
425	4.03	$988 - 18 i$	2.56	$989 - 3.74 i$
Local potential, Ref. [5]	18.6	$981 - 25 i$	unbound	–
Linear $\sigma$ model, Ref. [12]	–	$940 - 27 i$	–	$983.4 - 69 i$
Fermilab E 791 Collaboration [23]	–	$(975 \pm 3) - (22 \pm 2) i$	–	–
KLOE Collaboration [24]	–	–	–	$(984.8 \pm 1.2) - 61 i$
OBELIX Collaboration [25]	–	–	–	$(998 \pm 10) - 23 i$
Particle Data Group [11]	–	$(980 \pm 10) - (20 \text{ to } 50) i$	–	$(984.7 \pm 1.2) - (25 \text{ to } 50) i$

TABLE II: Bound state properties of the isoscalar potential: depth  $V_0$ , Eq. (15), effective mass ratio, Eq. (13), binding energy  $\epsilon_0$ , wave function at contact amplitude  $\psi(0)$ , and the factor  $R$  of Eq. (25).

$\Lambda$ (MeV)	$V_0(0)$ (GeV)	$M_K^*(0)/M_K$	$\epsilon_0$ (MeV)	$\psi(0)/M_K^{3/2}$	$R$
415	–0.23	2.18	21.3	0.126	1.041
420	–0.21	1.93	10.6	0.096	1.038
425	–0.19	1.75	4.03	0.072	1.034

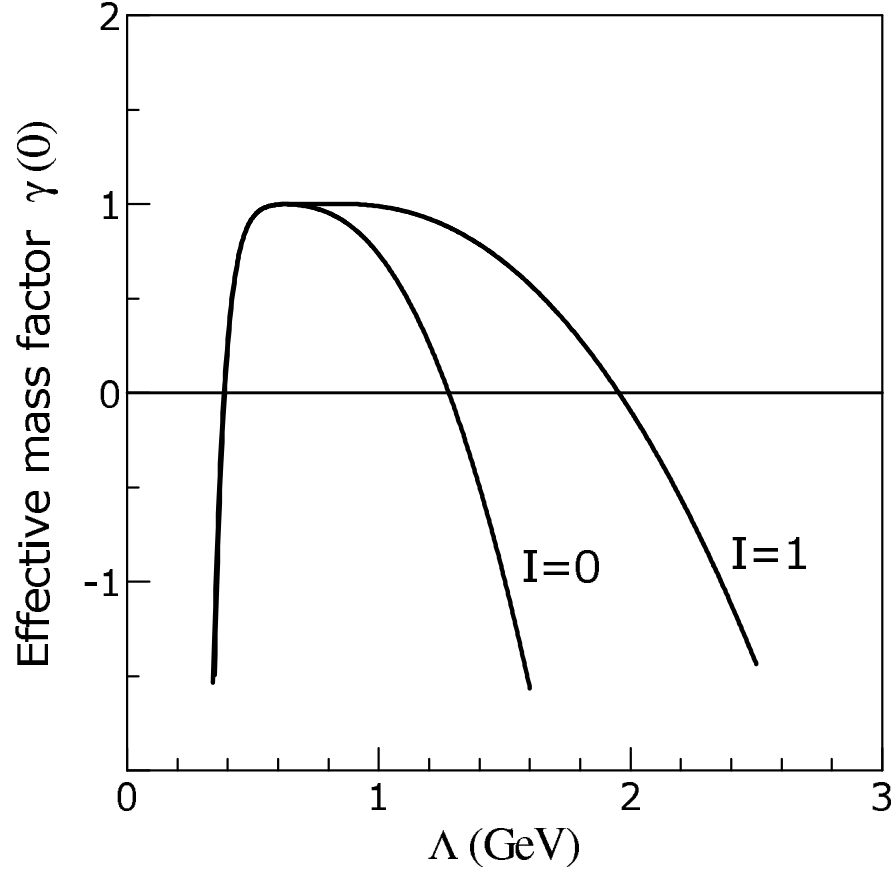


FIG. 1: Critical values of  $\gamma(0)$ , the inverse effective mass ratio versus the cutoff  $\Lambda$  for isospin  $I = 0$  and  $I = 1$ . Both curves remain positive in the common interval  $\sim 0.39 \lesssim \Lambda \lesssim 1.28$  GeV.

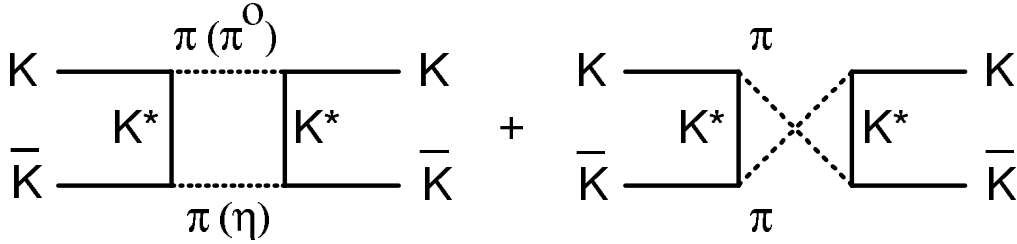


FIG. 2: The direct and exchange diagrams that contribute to the additional four-point vertex, or box diagram  $\hat{\Gamma}_{box}(\mathbf{p}', \mathbf{p}; P_0)$ , in the BS equation for  $K\bar{K}$  scattering that arises from  $t$ -channel  $K^*$ (892) exchange between the kaons, leading to  $\pi\pi$  isoscalar or  $\pi^0\eta$  isovector intermediate states. In the latter case only the first diagram is present.



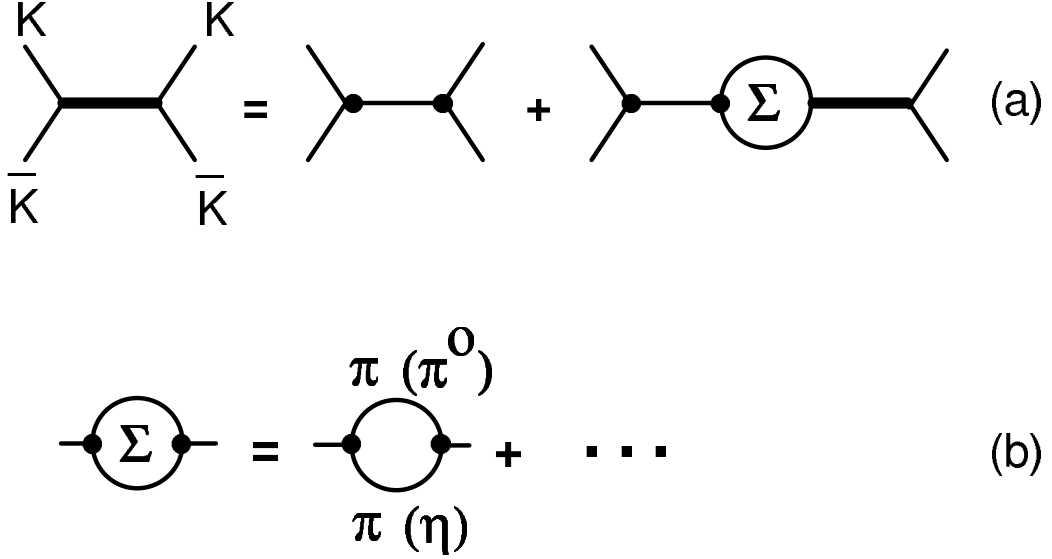


FIG. 3: (a) Meson exchange diagrams for  $s$ -channel contributions to the Bethe–Salpeter transition amplitude in Eq. (1). The thin and thick solid lines indicate bare versus dressed intermediate mesons propagating between interaction vertices, shown as filled circles. (b) The meson proper selfenergy  $\Sigma$ . Only the  $\pi\pi$  or  $\pi^0\eta$  polarization loop contributions to  $\Sigma$  that include imaginary parts for dressing the bare  $\sigma$  or  $a_0$  meson propagators at  $s = P_0^2 \approx 4M_K^2$  are shown.

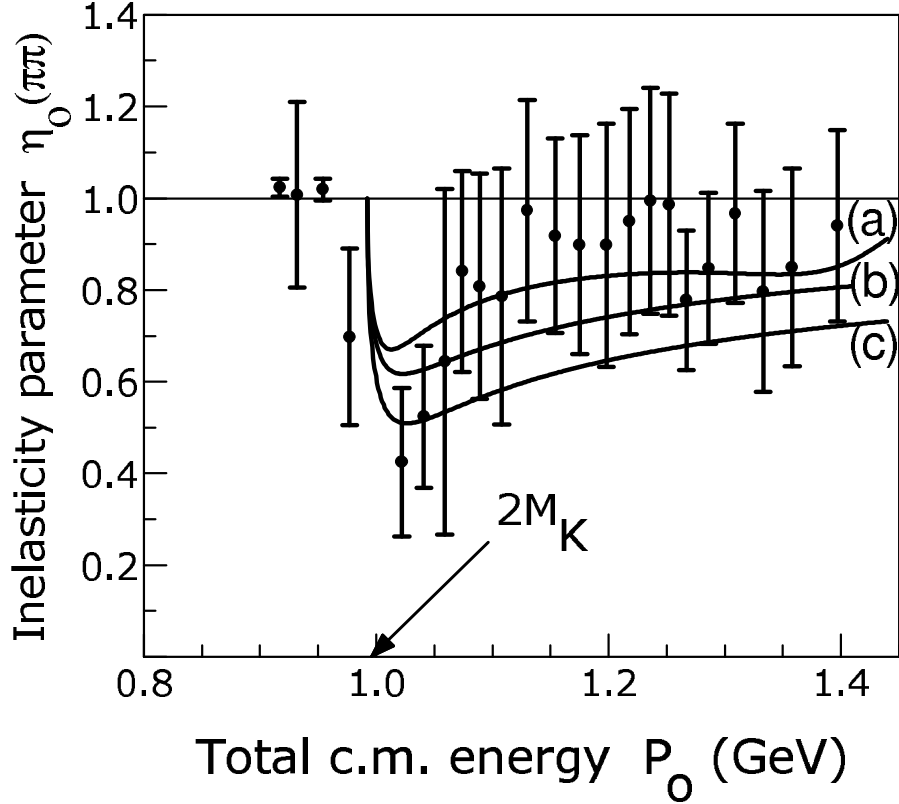


FIG. 4: The  $\pi\pi$  inelasticity versus the total center of mass (c.m.) energy. The filled circles with error bars show values of  $\eta_0(\pi\pi)$  taken from B. Hyams *et al.* [41], while the upper curve (a) gives the fit using the  $K$ -matrix from [42]. The lowest curve (c) shows the calculated inelasticity based on the effective range parameters of Eq. (41). Curve (b) gives the result using the scattering parameters for the local potential in [5].

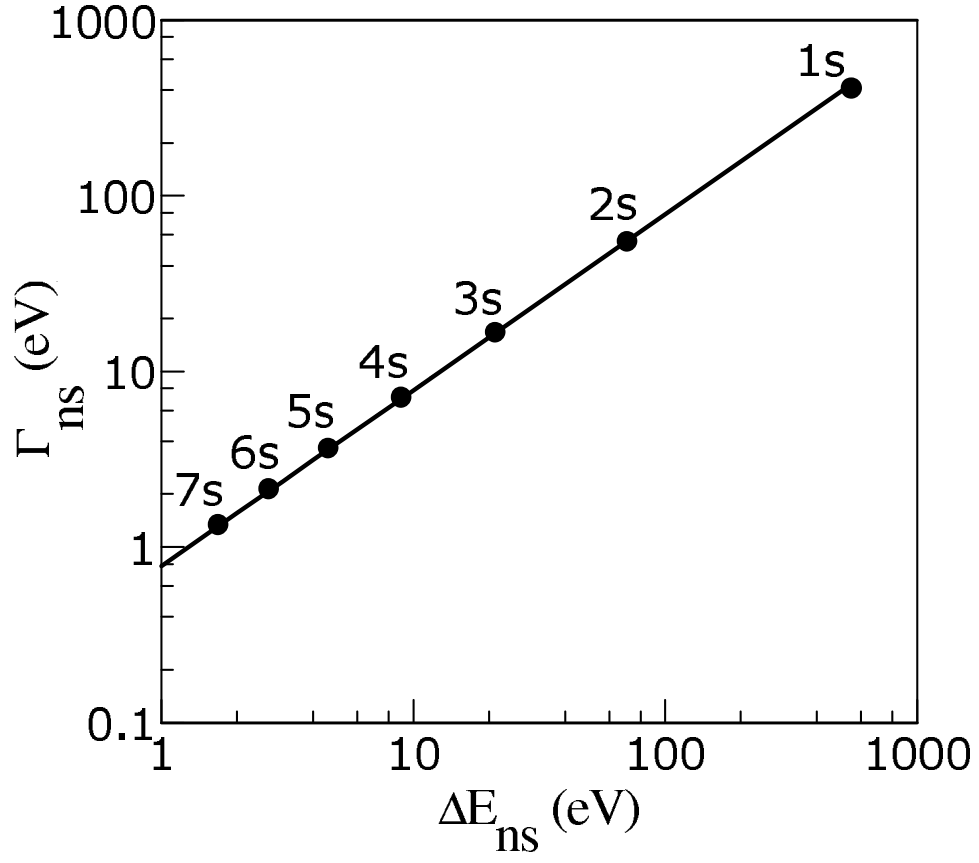


FIG. 5: Calculated decay widths  $\Gamma_{ns}$  versus the associated energy shifts  $\Delta E_{ns}$  for kaonium plotted on a log-log scale. The straight line is given by  $\Gamma_{ns} = 0.79\Delta E_{ns}$ .